

## Medium-energy ion-scattering analysis of the Cu(110) surface

M. Copel and T. Gustafsson

*Department of Physics, University of Pennsylvania, Philadelphia, Pennsylvania 19104-6396*

W. R. Graham and S. M. Yalisove

*Department of Materials Science and Engineering, University of Pennsylvania, Philadelphia, Pennsylvania 19104-6396*

(Received 23 December 1985)

A structural analysis of the interplanar spacing ( $d$ ) of the Cu(110) surface is reported, using medium-energy-ion scattering in a channeling and blocking experiment. Evidence is presented for a model with a multilayer oscillatory change in  $d$  with  $\Delta d_{12} = (-7.5 \pm 1.5)\%$  and  $\Delta d_{23} = (+2.5 \pm 1.5)\%$ . These values are in good agreement with those found with low-energy-electron diffraction but  $\Delta d_{12}$  is larger than that found by previous ion-scattering experiments. The model provides excellent agreement between data and Monte Carlo simulations.

### I. INTRODUCTION

One of the most important advances in surface crystallography in recent years has been the discovery that the interplanar spacings between atomic layers at a surface undergo oscillatory distortions. In most cases studied so far, the outermost interplanar spacing was found to be contracted, while the second layer spacing was expanded, in qualitative agreement with theoretical predictions for simple metals.<sup>1</sup> Experimentally, these effects have been observed both by low-energy-electron diffraction (LEED) and high-energy ion-scattering (HEIS). While there is general agreement about the existence and sign of these effects, quantitative disagreements have sometimes resulted when different experimental tools have been applied to the same system. A case in point is the Cu(110) surface, one of the first systems examined for multilayer contractions, and one of the few to which both LEED and HEIS have been applied. Two different LEED investigations<sup>2,3</sup> are in very good agreement, obtaining a large contraction of the spacing between the first and second layers ( $d_{12}$ ) and small expansion of the spacing between the second and third layers ( $d_{23}$ ) from the bulk value of 1.278 Å (Table I). It has been suggested<sup>2</sup> that the agreement between the two LEED studies was only limited by the choice of an appropriate reliability ( $R$ ) factor. This was further underscored by the spread of values quoted,<sup>2</sup> obtained by simply evaluating the same data set with different  $R$  factors. HEIS,<sup>4</sup> on the other hand, yielded  $\Delta d_{12} = -5.3\%$  and  $\Delta d_{23} = +3.3\%$ . These results differ not only in the actual magnitude of the changes, but there is also significant disagreement about the rate at which the changes decrease into the bulk. Theoretical studies of Al(110) have predicted a decrease in the distortion of the interplanar spacing with a relatively steep decay into the bulk.<sup>1</sup> It is obviously important to determine the scale of decay. Also, it is important to resolve differences between different structural techniques. We believed therefore that it would be useful to further investigate the surface geometry of Cu(110) in order to clarify these points. We report here a medium-energy ion-scattering (MEIS) study of the surface

geometry of Cu(110), using channeling and blocking, a technique not as widespread as either LEED or HEIS. A careful examination of the Ni(110) surface structure has been undertaken using MEIS for similar reasons and is the subject of another paper.<sup>5</sup>

In MEIS, as in HEIS, the backscattered flux of particles that have undergone Rutherford scattering<sup>6</sup> is measured. The incident beam (in our case, 100-keV protons) is aligned to a channeling direction of the target. Shadowing by surface atoms then greatly reduces the probability of collisions with the underlying substrate. In addition, the particles backscattered by the surface undergo fewer quasielastic losses to electrons than those that penetrate into the bulk. The resulting energy distribution is therefore dominated by a surface peak composed of particles that have not penetrated into the bulk. In a typical MEIS experiment, upwards of half of the detected ions in the surface peak originate in the first layer visible to the beam. The principle distinction between the experiments reported below and a typical HEIS measurement is that we have measured the angular distribution of the backscattered particles, while keeping the incident beam fixed in a channeling direction. The angular distributions are marked by blocking dips, where the surface atoms shadow backscattered particles from the second and third layers of atoms. A change of interplanar separation at the

TABLE I. Results for the change in layer spacing ( $\Delta d$ ) on Cu (110).

$\Delta d_{12}$ (%)	$\Delta d_{23}$ (%)	Reference	Technique
-10.0	+1.9	2 <sup>a</sup>	LEED
-7.9	+1.9	2 <sup>a</sup>	LEED
-9.5	+2.6	2 <sup>a</sup>	LEED
-8.5	+2.3	3	LEED
-5.3	+3.3	4	HEIS
-7.5	+2.5	Present work	MEIS

<sup>a</sup>The different results were obtained using different  $R$  factors on the same experimental data.

surface is observed as a shift in the position of the surface blocking dip away from the bulk crystallographic direction. Experimentally, MEIS can prove more complex than HEIS, in part because it involves angle-sensitive detection to measure blocking. In addition, a low beam energy optimizes the surface sensitivity, but it necessitates the use of an electrostatic energy analyzer instead of a simple solid-state detector.

The strength of MEIS, as well as HEIS, is that it is a *quantitative* probe. Since the cross section for Rutherford scattering is well known in this energy regime, the scattering yields can be converted to an absolute number of atomic scatterers per unit area. This makes it possible to simulate the scattering from an arbitrarily distorted crystal by a Monte Carlo calculation.

## II. EXPERIMENTAL

The measurements were performed in an ultrahigh-vacuum (UHV) chamber with operating pressures of less than  $2 \times 10^{-10}$  Torr. The scattering chamber<sup>7</sup> was connected to a 200 keV proton accelerator by a UHV differential pumping line so that the main vacuum system demonstrated no increase in pressure with a beam on target. MEIS depends critically on the ability to accurately detect both the position and the energy of protons backscattered from a sample. Ion energies were measured with a commercial toroidal electrostatic energy analyzer.<sup>8,9</sup> The total energy resolution, due to both the spread in incident proton energies and the contribution from the energy analyzer, was approximately 700 eV for 100 keV protons. This proved more than adequate for measuring a well-defined surface peak with little or no background when the sample was aligned to a channeling direction. The energy-analyzed ions were detected with channel plates and a position-sensitive detector which simultaneously measured an angular range of  $25^\circ$ , yielding an angular accuracy of  $\approx 0.2^\circ$ .

The backscattered yields were normalized using polycrystalline metal samples for random yield spectra. This calibration was limited by the accuracy of the literature values for the stopping power of the sample  $\partial E / \partial X$  used to evaluate random yields.<sup>10</sup> The number of neutralized backscattered protons was determined by measuring the ratio of ions to neutrals with a solid-state detector behind electrostatic deflection plates. We have used a neutralization probability of 22.6%, based on polycrystalline Ni, for our normalization. Previous MEIS studies have found similar values and have ascertained that no angular dependence exists in the neutralization probability.<sup>11</sup> We believe that this provides calibration of absolute yields to about 5%, and calibration of relative yields to a few percent. The beam dose per sample spot was kept below  $4 \times 10^{16}$  ions/cm<sup>2</sup>, although no beam-dose dependence was observed.

The sample was prepared by a combination of mechanical polishing, electropolishing, and a 200-h anneal at 900°C in a hydrogen atmosphere to leach out any residual sulfur contamination. The sample was then clamped into a copper holder, which permitted indirect heating by electron bombardment. It was cleaned *in situ* by several cy-

cles of Ne<sup>+</sup> sputtering and annealing. Surface cleanliness was monitored with LEED and retarding-field Auger spectroscopy. The annealing temperature was measured using an infrared pyrometer. The data in this paper were collected after flashing to  $\approx 450^\circ\text{C}$  and allowing the sample to cool for 1 h to a temperature of approximately 50°C. Data obtained after different annealing conditions did not show appreciably different relaxations. Once the sample had been aligned to the channeling direction ( $\pm 0.1^\circ$ ) and had been well annealed, it was found that realignment was rarely necessary after a sputter-anneal cycle.

Monte Carlo simulations of ion channeling and blocking have been described in the past,<sup>12</sup> and we will only point out a few features of the program used in the present study. We have performed a full crystal calculation that evaluates channeling and blocking independently. Our procedure includes a Rutherford term for angular effects that may occur by focusing during blocking. The program evaluates the probability of a collision with the atomic core with the impact parameter necessary to scatter the ion into the detector. The program makes use of a one-body isotropic vibration amplitude ( $u$ ). We have not included vibrational correlations of any kind in our calculations. Although correlation effects are doubtlessly important, in the two-body case it is possible to model correlation by a renormalized vibration amplitude.<sup>13</sup> In the simulations included in this paper, it was found to be unnecessary to go to a depth greater than four atoms along any atomic row (a four- or eight-layer calculation depending on the geometry). Thus we feel justified in using a two-body renormalization to approximate full correlations. The strategy of using an uncorrelated vibration, and then renormalizing to approximate correlations, has been applied successfully in a previous MEIS study.<sup>11</sup> For the remainder of this paper, the following convention will be used: All vibration amplitudes will refer to uncorrelated, one-dimensional values. All calculated Debye temperatures will include an estimated correlation.

## III. RESULTS

We have obtained data for 100-keV protons incident in two different experimental geometries. Figure 1 shows a top view of the Cu(110) surface indicating the two scattering planes, as well as side views.

The first scattering geometry is a  $(\bar{1}11)$  plane with channeling in a  $[0\bar{1}1]$  direction and blocking in a  $[101]$  direction ( $[0\bar{1}1]_{\text{ch}}$ ,  $[101]_{\text{bl}}$ ). Here, if we were able to confine the copper atoms to a static lattice, we would find only the first layer of atoms visible to the incident beam. With the addition of vibrations the second layer becomes visible. Consequently, we expect this geometry to be chiefly a measure of  $\Delta d_{12}$ .

The second scattering geometry is a (001) plane with channeling in the  $[\bar{1}00]$  direction and blocking in the  $[010]$  direction. With this incidence direction, the ion beam would hit both the first and second layers of a static lattice, encountering two inequivalent scattering planes. The plane terminated by the first layer also contains the third and subsequent odd-numbered layers. The backscattered

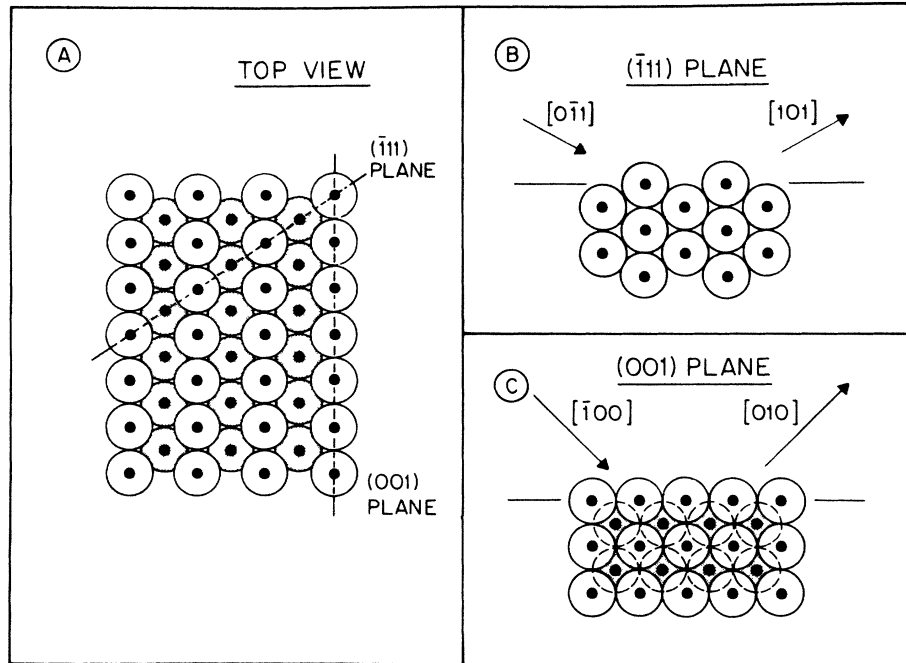


FIG. 1. Views of the Cu(110) surface. (a) Top view. The second-layer atoms are shaded. (b) The  $(\bar{1}11)$  plane, showing channeling and blocking directions. (c) The  $(001)$  plane, showing the two inequivalent scattering planes, one terminating in the top layer, the other in the second layer.

flux from the third layer will be blocked by atoms in the first layer. Angular shifts from this plane will contain information about  $\Delta d_{13}$ . The second set of planes is terminated by the second layer, and contains atoms in even-numbered layers. Scattering from this plane will therefore be a measure of  $\Delta d_{24}$ . The data from this geometry therefore depends on  $\Delta d_{13} + \Delta d_{24}$ .

In order to assess the agreement of the data with the Monte Carlo simulations, we have used an  $R$  factor analysis. In keeping with earlier work,<sup>4</sup> a scaled  $R$  factor was defined as follows:

$$R = (100/N) \left[ \sum (wY_{\text{expt}} - Y_{\text{calc}})^2 / (wY_{\text{expt}})^2 \right]^{1/2},$$

where  $Y_{\text{expt}}$  ( $Y_{\text{calc}}$ ) is the experimental (calculated) scattering yield at a particular angle,  $w$  is a scaling constant, and the summation is to be carried out over the  $N$  measured data points in a blocking dip. The scaling constant  $w$  was used to reduce the importance of absolute accuracy in the normalization of the calculations, and serves to emphasize the importance of angular shifts. In our final model the scaling constants for the two geometries are 1.01 and 1.02. It is possible to calculate an overall  $R$  factor for more than one geometry by summing the  $R$  factor over all data points collected. We will refer to this as a total  $R$  factor.

A surface blocking dip for the  $[0\bar{1}1]_{\text{ch}}$ ,  $[101]_{\text{bl}}$  configuration is shown in Fig. 2, along with our best-fit simulation. Here the data have already been normalized to the Rutherford cross section, including an angle-independent screening term.<sup>14</sup> The angular shift from the bulk  $[101]$  direction is  $-1^\circ$  (negative numbers indicate a shift towards smaller scattering angles), which would translate to a contraction of  $d_{12}$  by about 4%, if one were to consider the scattering from only the first two layers. However,

such a simple analysis neglects the strong contributions from lower layers that may occur for a surface with a low Debye temperature. Scattering from deeper layers in the crystal has the effect of bringing the blocking dip to the bulk value, i.e., towards larger scattering angles. Thus a strongly vibrating crystal may undergo a much larger contraction than one would expect from just examining the shift in the blocking dip. The minimum of the surface blocking dip in Fig. 2 is at 1.55 monolayers, significantly higher than the 1.35 monolayers found in the same geometry on Ni(110).<sup>5</sup> We attribute this to a higher

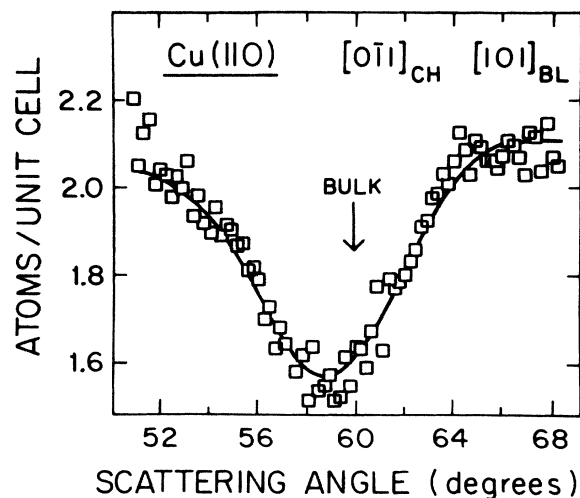


FIG. 2. Blocking dip in the  $(\bar{1}11)$  plane in the geometry of Fig. 1(b) for 100 keV protons. The bulk blocking direction is at  $60^\circ$ . A contraction will cause a shift to smaller scattering angles. The solid curve is a Monte Carlo simulation for  $\Delta d_{12} = -7.5\%$  and  $\Delta d_{23} = +2.5\%$ .

thermal vibration amplitude on the Cu(110) surface. If we were to restrict ourselves to using a single Debye temperature for both the bulk and the surface in fitting our data, this value would be 0.097 Å, much greater than the value of 0.07 Å used for all layers on Ni(110).

In Fig. 3 we present a contour plot of the scaled  $R$  factor for scattering in the  $[\bar{1}11]$  plane that was calculated by use of the Monte Carlo simulation. In this calculation the scaling constant varied between 0.96 and 1.05. The two axes are the interplanar spacings of the first two layers. It can be seen that there is some sensitivity to second-layer movements in this geometry.

Data from the second geometry, the (001) zone, along with the Monte Carlo simulation for the best-fit model, are shown in Fig. 4. The surface blocking dip shows an angular shift significantly smaller than in Fig. 2, indicating that  $\Delta d_{12}$  and  $\Delta d_{23}$  have opposite signs. In Fig. 5 we show a contour map of the  $R$  factor for the (001) zone as a function of the first two interplanar spacings. In this calculation the scaling constant varied between 0.99 and 1.06. The minimum  $R$  factor defines a trough that cuts across the graph. The slope of the trough reflects the fact that we are measuring  $\Delta d_{13}$  and  $\Delta d_{24}$  with approximately equal weighting. When attempting to model the crystal with a single vibration amplitude, these data were best fitted by an amplitude of 0.085 Å, somewhat smaller than the value of 0.097 Å found in the  $[\bar{1}11]$  plane. The reason for this difference is that the (001) geometry probes deeper into the crystal, and hence the vibrations are more bulk-like.

Obviously, it is unsatisfactory to use different vibrational amplitudes in the two different scattering geometries. Instead, we have used a model with two vibration amplitudes: a bulk amplitude and a larger surface amplitude.<sup>11</sup> The latter decays exponentially into the bulk with a decay constant equal to one interplanar spacing. The best fit for the combination of both geometries is given by a bulk vibration amplitude of 0.072 Å and an enhancement of the surface vibrations by 55%. The bulk

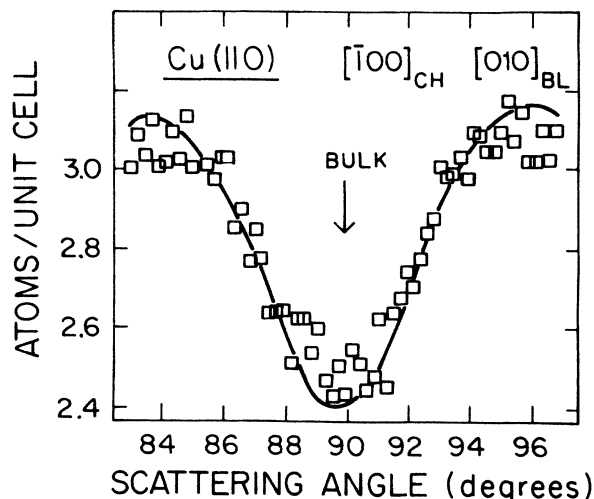


FIG. 4. Blocking dip in the (001) plane in the geometry of Fig. 1(c) for 100 keV protons. In this plane, both the first and second layers of the surface are directly visible to the incident beam. The bulk blocking direction is at 90°. The solid curve is a Monte Carlo simulation for  $\Delta d_{12} = -7.5\%$  and  $\Delta d_{23} = +2.5\%$ .

Debye temperature of Cu is approximately 320 K. This corresponds to  $u = 0.072$  Å for our crystal temperature of  $\approx 320$  K, assuming a correlation coefficient of 0.3 (Ref. 4). The surface Debye temperature, assuming the same correlation as the bulk, is then 205 K. Both the contour maps and the best fits shown in this paper use these values for thermal vibration amplitudes.

In Fig. 6 we display the total  $R$  factor for both geometries as a function of vibrational enhancement. In this case, the scaling constant has been confined to 1.00 (i.e., an unscaled  $R$  factor). There is a clear minimum for the enhancement given above. Performing the same analysis for each blocking dip independently, the data are best fitted by a 60% enhancement in the  $(\bar{1}11)$  plane and

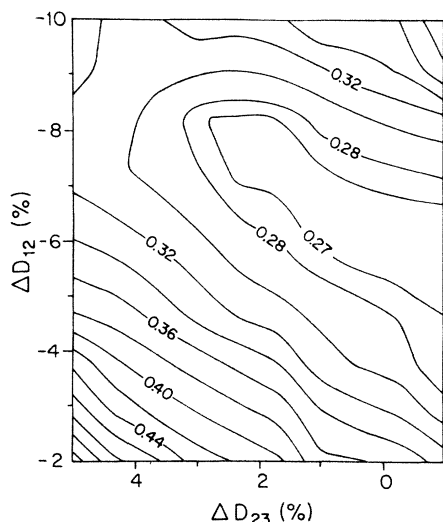


FIG. 3. Contour map of the  $R$  factor for the  $(\bar{1}11)$  geometry as a function of the first and second interplanar spacings.

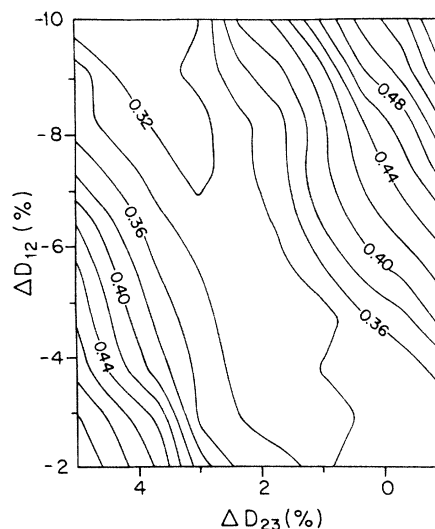


FIG. 5. Contour map of the  $R$  factor for the (001) geometry as a function of the first and second interplanar spacings.

TABLE II. Vibrational parameters of selected fcc (110) surfaces, measured by ion scattering.

Surface	Technique	Ref.	Bulk Debye Temp. (K)	Surface Debye Temp. <sup>a</sup> (K)	Vibrational Amplitude Enhancement <sup>a</sup> (%)
Ni(110)	HEIS	15	375	325	15
	MEIS	5		355	
Ag(110)	HEIS	16	215	149	44
Cu(110)	HEIS	4	320	250	27
	MEIS	17	315	250	25
	MEIS	Present work	320	205	55

<sup>a</sup>See the text for details of the way the surface enhancement of the vibrational amplitudes was modeled in different studies.

50% in the (001) plane, in very satisfying internal agreement.

It is not straightforward to compare our values for the vibrational enhancements with those found by others (Table II) due to the different ways such enhancements have been modeled in the literature. In a HEIS study of Ni(110) the data were analyzed with a bulk Debye temperature of 375 K and an enhancement restricted to the first layer of atoms.<sup>15</sup> This resulted in a surface Debye temperature of 325 K, i.e., an enhancement of the amplitude by 15%. In a recent MEIS study<sup>5</sup> of the same surface, the data were analyzed with a single Debye temperature of 355 K. HEIS data on Ag(110) (Ref. 16) yielded an enhancement of the first-layer vibrations of  $\approx 44\%$ , again using a model where the vibrations of only the first layer of the crystal were enhanced. Analyses of earlier ion-scattering experiments on Cu(110) have either used the same exponentially decaying surface enhancement as in the present analysis,<sup>17</sup> or restricted the enhancement to the first layer only,<sup>4</sup> just as for Ni(110).<sup>15</sup> This resulted in models with enhancements in the range of 25%, not very different from the results for Ni(110).<sup>5,15</sup> As discussed above, there is a strong interdependence between vibra-

tional amplitudes and the surface specificity of a given ion-scattering experiment. Therefore, a larger surface enhancement implies a larger contribution to the ion-scattering yield from deeper layers, which in turn implies a larger first-layer contraction for a given angular shift. We believe that this is sufficient to account for the differences between the structural models in our work and previous ion-scattering experiments.<sup>4,17</sup> In earlier work, restricted to the  $(\bar{1}11)$  zone, a lower yield was measured in double alignment, and was modeled with a smaller change in  $d_{12}$ , keeping  $d_{23}$  fixed.<sup>17</sup>

We have calculated the total  $R$  factor in Fig. 7. The minimum of the total  $R$  factor plot lies at the intersection of the two troughs that appear in the contour maps for the two different geometries. The contours formed by the total  $R$  factor are not, however, circular. There is instead a pronounced asymmetry in the contours, indicating sensitivity to the sum of the displacements of the first two layers. This can be expressed as  $\Delta d_{12} + \Delta d_{23} \approx -5\%$ . Similar equations have been obtained in Refs. 5 and 16, both of which used unscaled  $R$  factors and varied the Debye temperature.

The final result of the analysis is a model in which the

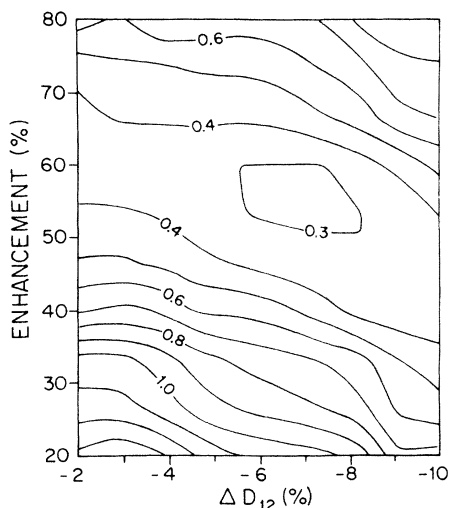


FIG. 6. Contour map of the (unscaled) total  $R$  factor as a function of the first interplanar spacing and the enhancement of the surface vibration amplitude.

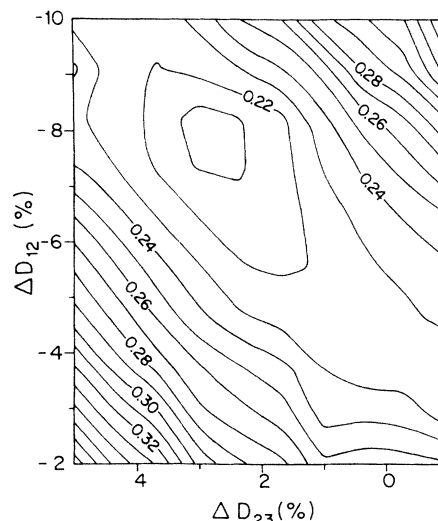


FIG. 7. Contour map of the total  $R$  factor as a function of the first and second interplanar spacings. The minimum lies at the best fit for the data,  $\Delta d_{12} = -7.5\%$ ,  $\Delta d_{23} = +2.5\%$ .

first interplanar spacing is contracted by  $(7.5 \pm 1.5)\%$  and the second interplanar spacing is expanded by  $(2.5 \pm 1.5)\%$ . A visual assessment showed poor agreement between data and simulations for models outside of the stated error bars. The error margins have been estimated by examining the sensitivity to a 5% change in absolute normalization. This normalization is the largest source for errors in the structural model. A change in normalization would imply different vibrational amplitudes and, in turn, different structural parameters. For example, if the normalization were to change 20% in the direction resulting in a smaller yield, we would calculate a relatively small enhancement of the vibrations and a first-layer contraction of only about 4%.

#### IV. CONCLUSIONS

We have performed a structural analysis of the interplanar spacing of the Cu(110) surface, and found evidence for a multilayer oscillatory relaxation with  $\Delta d_{12}$

$=(-7.5 \pm 1.5)\%$  and  $\Delta d_{23}=(+2.5 \pm 1.5)\%$ . Compared to other results (Table I), the present model is in excellent agreement with earlier LEED results.<sup>2,3</sup> Our results remove the discrepancy between LEED and earlier ion-scattering results.<sup>4</sup> The decrease in the amplitude of  $\Delta d$  with depth is in keeping with that predicted for Al(110).<sup>1</sup>

We have also found evidence of a large ( $\approx 55\%$ ) enhancement of the thermal vibration amplitude on the Cu(110) surface. Our observation of this enhancement is a direct consequence of the difference in depth sampled in the  $(\bar{1}11)$  and (001) planes.

#### ACKNOWLEDGMENTS

This research was supported by the National Science Foundation (NSF) under Grants Nos. DMR-80-15302 (M.C. and T.G.), DMR-83-12006 (W.R.G. and S.M.Y.), and DMR-82-16718. The acquisition of the toroidal analyzer was made possible by NSF Grant No. DMR-83-09652.

<sup>1</sup>U. Landman, R. N. Hill, and M. Mostoller, Phys. Rev. B **21**, 448 (1980); R. N. Barnett, U. Landman, and C. L. Cleveland, *ibid.* **27**, 6534 (1983).

<sup>2</sup>H. L. Davis and J. R. Noonan, Surf. Sci. **126**, 245 (1983).

<sup>3</sup>D. L. Adams, H. B. Nielsen, and J. N. Andersen, Surf. Sci. **128**, 294 (1983).

<sup>4</sup>I. Stensgaard, R. Feidenhans'l, and J. E. Sørensen, Surf. Sci. **128**, 281 (1983).

<sup>5</sup>S. M. Yalisove, W. R. Graham, E. D. Adams, M. Copel, and T. Gustafsson, Surf. Sci. (to be published).

<sup>6</sup>L. C. Feldman, J. W. Mayer, and S. T. Picraux, *Materials Analysis by Ion Channeling* (Academic, New York, 1982).

<sup>7</sup>W. R. Graham, S. M. Yalisove, E. D. Adams, T. Gustafsson, M. Copel, and E. Törnqvist, Nucl. Instrum. Methods (to be published).

<sup>8</sup>R. G. Smeenk, R. M. Tromp, H. H. Kersten, A. J. H. Boerboom, and F. W. Saris, Nucl. Instrum. Methods **195**, 581 (1982).

<sup>9</sup>R. M. Tromp, H. H. Kersten, E. Granneman, F. W. Saris, R. Koudjis, and W. J. Kilsdonk, Nucl. Instrum. Methods B **4**, 155 (1984).

<sup>10</sup>H. H. Andersen and J. F. Ziegler, *The Stopping and Ranges of Ions in Matter* (Pergamon, New York, 1977), Vol. 3.

<sup>11</sup>J. W. M. Frenken, R. G. Smeenk, and J. F. van der Veen, Surf. Sci. **135**, 147 (1983).

<sup>12</sup>I. Stensgaard, L. C. Feldman, and P. J. Silverman, Surf. Sci. **77**, 513 (1978).

<sup>13</sup>D. P. Jackson and J. H. Barrett, Comput. Phys. Commun. **13**, 157 (1977).

<sup>14</sup>A. Weber, H. Dahlmann, H. Mommsen, and W. Sarter, Nucl. Instrum. Methods **200**, 567 (1982).

<sup>15</sup>R. Feidenhans'l, J. E. Sørensen, and I. Stensgaard, Surf. Sci. **134**, 329 (1983).

<sup>16</sup>Y. Kuk and L. C. Feldman, Phys. Rev. B **30**, 5811 (1984).

<sup>17</sup>M. Copel, W. R. Graham, T. Gustafsson, and S. Yalisove, Solid State Commun. **54**, 695 (1985).

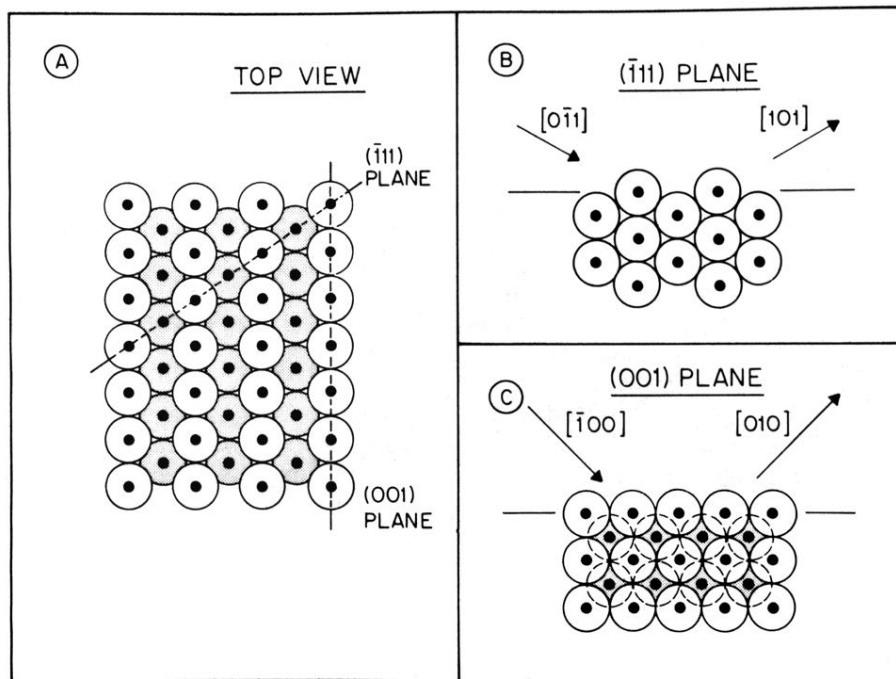


FIG. 1. Views of the Cu(110) surface. (a) Top view. The second-layer atoms are shaded. (b) The  $(\bar{1}11)$  plane, showing channeling and blocking directions. (c) The (001) plane, showing the two inequivalent scattering planes, one terminating in the top layer, the other in the second layer.